

Supplementary Information:

Controlling droplet transport to target on a gradient adhesion surface

Shile. Feng,^a Sijie. Wang,^a Chengcheng. Liu,^a Yongmei. Zheng^{*a} and Yongping. Hou^{*a}

Experimental section:

Modification of the graphite plate: A graphite plate with low density (size of 30×10×3 mm manufactured by Ji Xing Sheng An Co. (Beijing, China)) was perpendicularly inserted into electrolyte (T: top part and B: bottom part) and treated via improved anodic oxidation (AO) as previously reported.⁵ Position zero was chosen to be the top point of graphite plate. Then the graphite plate was modified with Octafluorocyclobutane (C₄F₈) plasma (AOP) via Inductively Coupled Plasma Etching System (ICP-98A, Institute of Microelectronics of the Chinese Academy of Sciences). The radio-frequency power of plasma etching was 30 Kw and the processing time was 2 min. The flow rate was controlled at 200 SCCM (standard-state cubic centimeter per minute) to set the plasma pressure of 5 Pa.

After AOP treatment, the graphite plate possesses controlled adhesion gradient (from ultrahigh to ultralow) and anisotropic adhesion. Generally, the water adhesive property on a surface is mainly governed by two factors: the surface geometrical structure and chemical composition. Consequently, by dynamically adjusting the two factors, the water adhesion could be effectively tuned. Firstly, we control the surface morphology and chemical composition via current gradient and oxidation time gradient. The bottom areas have smoother morphology and more oxygen-containing surface groups as mentioned above (Scheme 1a) due to the increase of current and oxidation time from top areas to bottom ones, forming a large wettable gradient of 3.2°/mm. Then, during the plasma treatment process, fluorine and fluorocarbon radicals would be produced. Based on the fact that the atomic ratio of F/C is very lower (the maximum is only 0.06) and the atomic ratio of O/C changes a little compared with the ratio on S-AO, it is inferred that the oxygen-containing surface groups do not change but only fluorine substitutes for α -hydrogen (high active) from side chain of phenyl ring, just a softer functionalization.³³ As said above, the current gradient leads to more oxidative benzene fracture at bottom areas, therefore, the content of F element increases from top areas to bottom ones, exhibiting a gradient. As the introducing of F would decrease the surface energy of graphite plate, the direction of wettable gradient is reverse and the surface of AOP sample becomes hydrophobic. Therefore, after AOP, the contact state can be tuned between the Wenzel state with high adhesion to

the Cassie state with low adhesion via adjusting the microstructures and chemical composition, showing an adhesion gradient from ultrahigh to ultralow (Scheme 1b).

Characterization: Water contact angles (CAs) and SAs were measured by the optical contact angle meter system (OCA40Micro, Dataphysics Instruments GmbH, Germany). A 5.0 μ L of deionized water was dropped onto the samples and the static CA and SA were determined by the average of at least five measurements. The adhesion force was measured by surface interface tensiometer (DCA21, Dataphysics, Germany). Scanning electron microscopy (SEM) equipped with energy dispersive spectrometer (EDS) (JSM-6500F, JEOL) was employed for the microstructure and chemical composition identification of graphite plate surface after AO or AOP treatment. The horizontal vibration was exerted on graphite plate via a vibrator (LONGDATE, China). The directional movement behaviors of droplets were observed by a high speed CCD (HSCCD, V9.1, PHANTOM, America). An atomic force microscopy (AFM, Bruker Icon) was performed with tapping mode to in-situ analyze the surface roughness of original and treated graphite plate. The used frequency of probe (SNL-10A) is 66.3 kHz. The roughness was estimated with the root-mean-square (RMS) roughness by analyst provided in AFM software system.

Supplementary Figure Legend: Fig. S1-S6

Fig. S1:

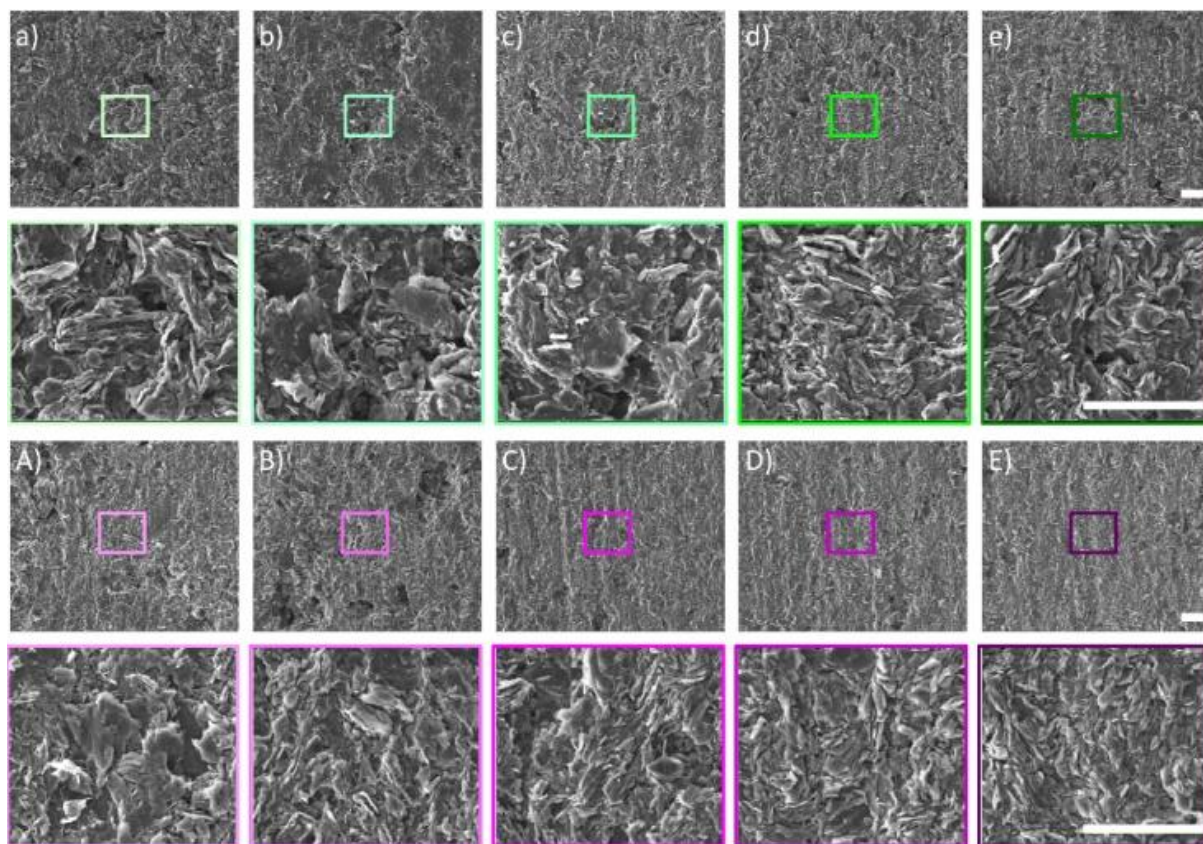


Fig. S1 SEM images of graphite plate at different areas. **a-e**) After AO treatment. **a)** 5 mm, **b)** 10 mm, **c)** 15 mm, **d)** 20 mm and **e)** 25 mm (distance from top to bottom). **A-E)** After AOP treatment. Corresponding SEM images of (**a-e**) respectively. It is clear that after AO treatment, the roughness gradient is formed. After AOP treatment, the roughness gradient is reserved, only the whole surface becomes smooth. Scale bars, 30 μm .

Fig. S2:

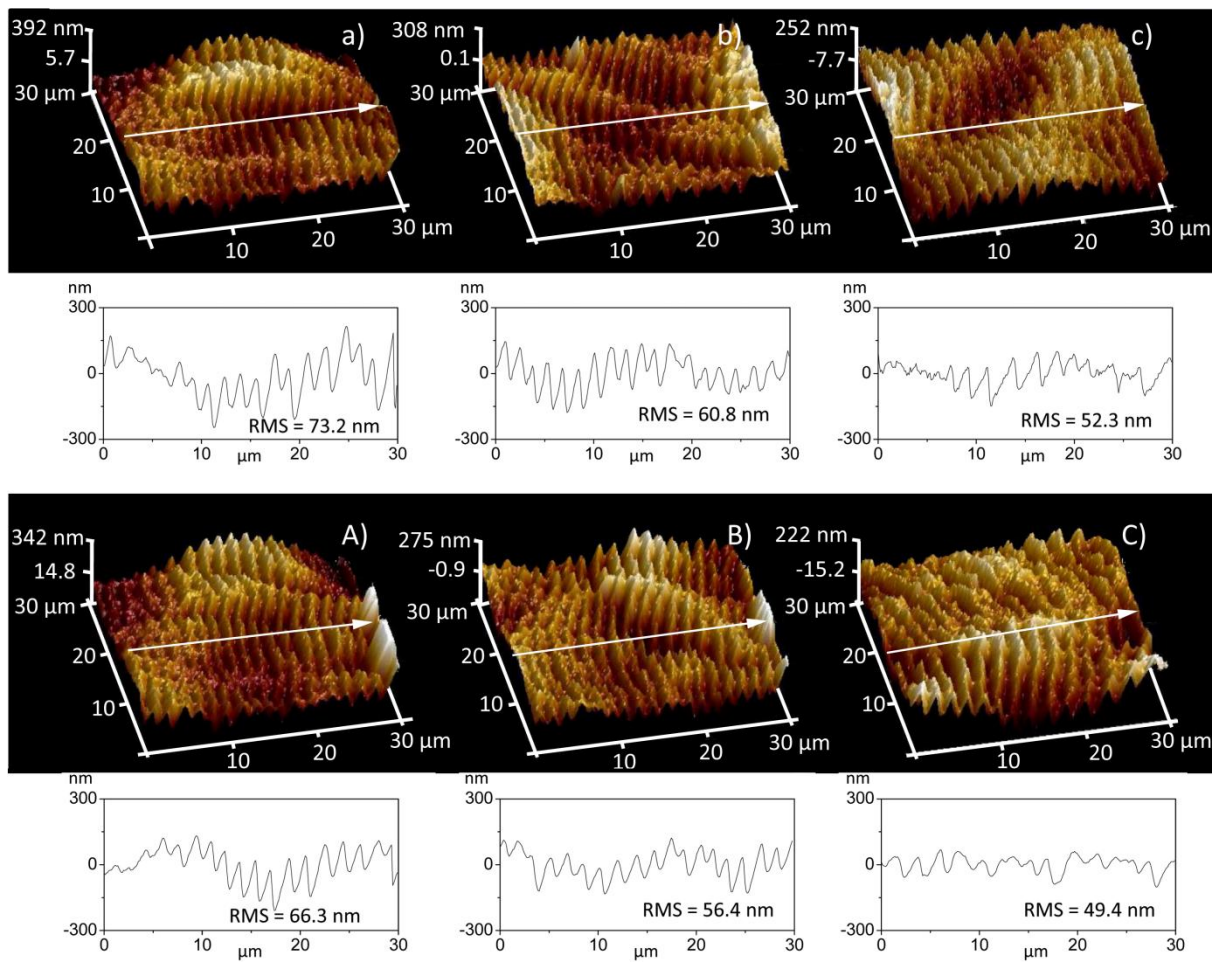


Fig. S2 AFM images of graphite plate at different areas. **a-c)** After AO treatment. **a)** 5 mm, **b)** 15 mm and **c)** 25 mm (distance from top to bottom). The root-mean-square (RMS) roughness of the S-AO changes from ~ 73.2 nm to ~ 52.3 nm. **A-C)** After AOP treatment. Corresponding SEM images of **(a-c)** respectively. The RMS roughness of the S-AOP decreases from ~ 66.3 nm to ~ 49.4 nm.

Fig. S3:

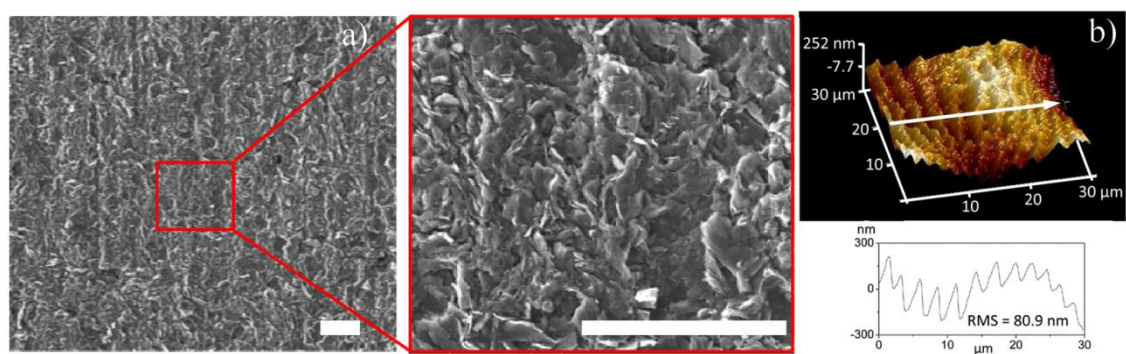


Fig. S3 a) SEM morphology of original graphite plate. Scale bars, 30 μm . **b)** AFM morphology of original graphite plate. There is the root-mean-square (RMS) roughness of ~ 80.9 nm.

Fig. S4:

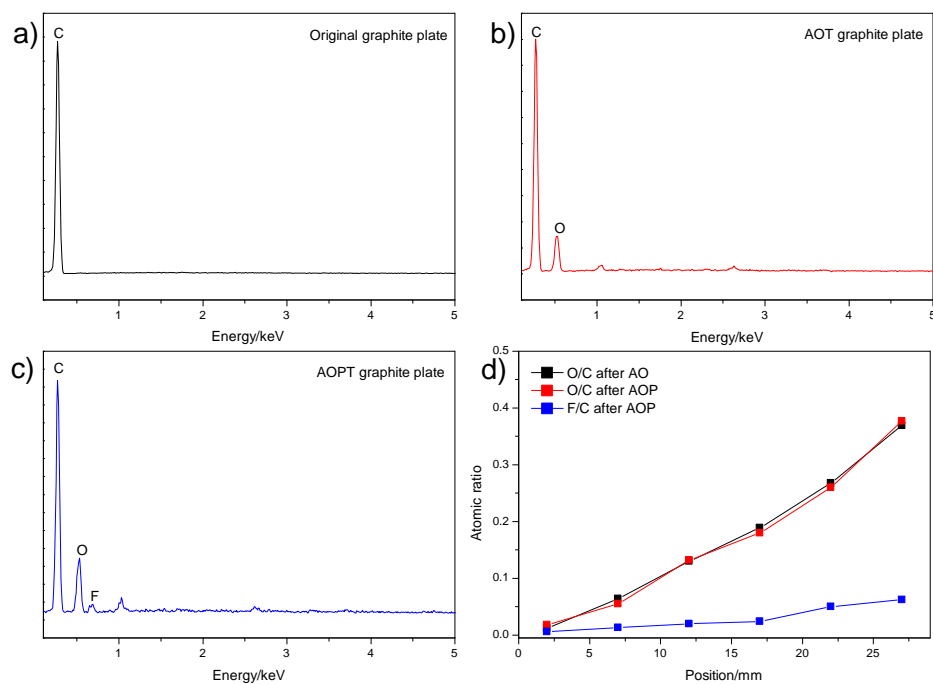


Fig. S4 a-c) Typical EDS spectra of **a)** original graphite plate, **b)** graphite plate after AO, **c)** graphite plate after AOP. **d)** Atomic ratio obtained from EDS spectra on different areas after AO and AOP. It is clear that after AO and AOP treatment, the O and F element content gradient are formed.

Fig. S5:

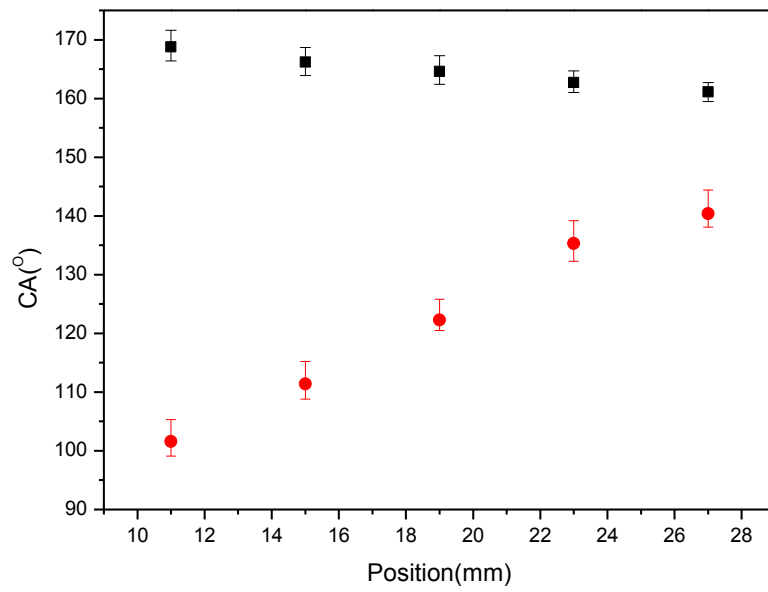


Fig. S5 The advancing CAs (■ scatter) and receding CAs (● scatter) in the different areas of the AOP graphite plate along the wettability direction.

Fig. S6:

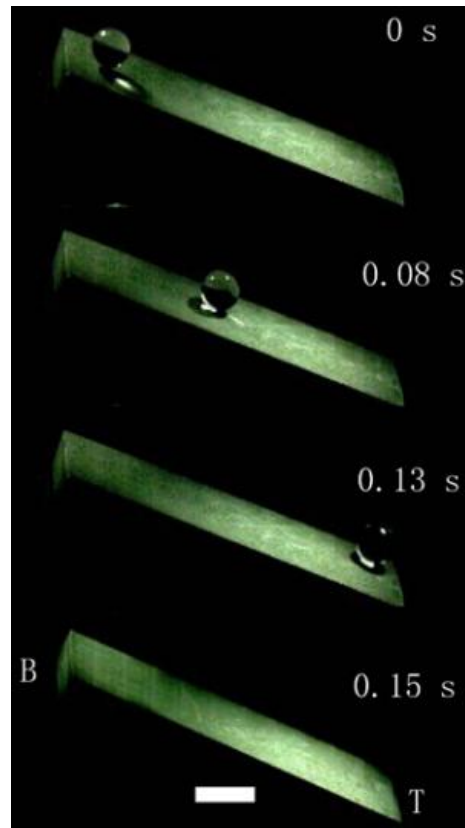


Fig. S6 The sliding behaviors of water droplets at tilted angle of 16.2° . At this condition, the water droplets would slide off from the graphite plate. The scale bar is 5 mm and the volume of the water droplet is $10 \mu\text{L}$.

Table S1. The sliding distances of droplets on surfaces along the wettability gradient based on experiment and calculation at different tilted angles of surface.

Tilted angle [°]	5	7	9	12
Actual measured value [mm]	7.38	11.29	15.23	21.23
calculated value [mm]	7.44	11.7	16.55	21.86